CP955, *Shock Compression of Condensed Matter - 2007,*
edited by M. Elert, M. D. Furnish, R. Chau, N. Holmes, and J. Nguyen

NEW OPTICAL DIAGNOSTICS FOR EQUATION OF STATE EXPERIMENTS ON THE JANUS LASER

D. K. Spaulding[1], D. G. Hicks[2], R. F. Smith[2], J. H. Eggert[2], R. S. McWilliams[1,2], G. W. Collins[2], and R. Jeanloz[1]

[1]*Department of Earth and Planetary Science , University of California, Berkeley, CA 94720-4767*
[2]*Lawrence Livermore National Laboratory, Livermore, CA 94550*

Abstract. We describe the configuration of two new optical diagnostics for laser-driven dynamic-compression experiments to multi-Mbar pressures. A streaked optical pyrometer (SOP) has been developed to provide temporally and spatially-resolved records of the thermal emission from shock-compressed samples. In addition, temporally-resolved broadband reflectivity is measured between 532 and ~850 nm by supercontinuum generation in an optical fiber. These new tools expand capabilities to probe the thermal and electronic states of matter at high pressures and temperatures using the Lawrence Livermore National Laboratory's Janus laser.

Keywords: Temperature, optical absorption, pyrometer, laser-driven acceleration.
PACS: 78.20.Ci, 07.20.Dt, 07.20.Ka, 41.75.Jv.

INTRODUCTION

Laser-driven dynamic compression experiments are increasingly being applied to characterize materials at ultra-high temperatures and pressures. Such experiments typically use velocity interferometry to infer the kinematic properties (pressure (P), density (ρ), energy (E)) of the equation of state (EOS), however the thermal and optical properties of materials are not as widely characterized under such conditions, and have historically proven difficult to obtain. Complete pressure-volume-temperature EOS data, and studies of the electronic and optical properties of materials demand additional diagnostics to allow such phenomena as phase transitions, band-gap closure and changes in chemical-bonding character to be documented. Here we describe the basic experimental configuration for two new high time-resolution optical diagnostics at the Janus laser: a streaked optical pyrometer for absolute temperature determination, and a nanosecond broadband reflectivity diagnostic for studies of the electronic and optical properties of materials.

EXPERIMENTAL CONFIGURATION

Janus is a two-beam Nd:glass laser (1kJ/beam at 1ω, or 1053nm) operated at the Jupiter Laser Facility at Lawrence Livermore National Laboratory. The diagnostics described herein are designed to complement and be fielded simultaneously with existing systems, including a two-channel VISAR (Velocity Interferometer for Any Reflector) and existing single-wavelength reflectivity capabilities for laser-driven shock and ramp-compression experiments.

In a typical experiment, the sample is mounted on a thin aluminum pusher in which a shock is ablatively developed by a single pulse (527nm, 2ω) laser drive, adjustable between 250 ps and 20 ns in

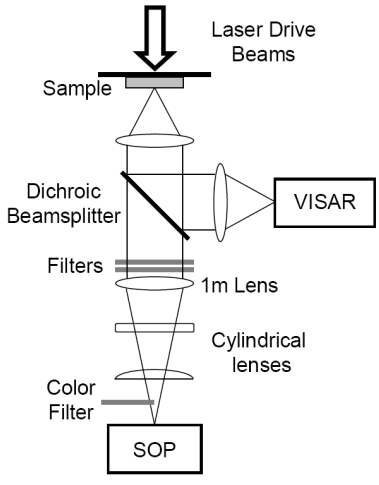

FIGURE 1. Self-emission from the sample is separated from the VISAR signal by a dichroic beamsplitter, and focused onto the SOP streak camera by the optical train described in the text.

duration. The diagnostics observe the face of the sample opposite the drive, where the probes and thermal emission are conveyed out of the evacuated sample chamber to the detectors.

Streaked Optical Pyrometry

Thermal emission is collected by streaked optical pyrometry to determine the temperature of the compressed material . Because the pyrometer is run in parallel with the VISAR, a common collection objective-assembly focuses the interferometer probe-beam onto the sample, and collects and collimates the returning signal along with the thermal emission (Fig. 1). The lens assembly is approximately f/3, with a focal length of 146 mm and a lens aperture of 5 cm. A 45 degree dichroic beamsplitter centered at 532 nm separates the VISAR probe from the wavelengths measured by the pyrometer. Outside the target chamber, the thermal emission is focused onto a Hamamatsu C7700 streak camera [1] by means of a 1 m achromat and two cylindrical lenses (500 mm plano-concave and 100 mm plano-convex) that serve to compress the image of the sample perpendicular to the opening (slit) aperture of the camera. The resulting magnification is a factor of 8 along the aperture, resulting in a spatial resolution of ~12 μm/pixel across the sample. Time resolution is typically ~100 ps for our experiments, and is determined by the sweep rate and aperture of the streak camera. A holographic notch filter centered at 532 nm is used in the collimated portion of the pyrometer beam-path for additional rejection of the VISAR signal, and a set of calibrated neutral-density filters can be applied to accommodate intense signals without saturating the camera. The magnification, alignment and focus are checked prior to a given experiment by placing a grid of known spacing in the target plane.

The spectral response of the pyrometer, $S(\lambda)$, is modulated by the transfer function of the optics described above and, most significantly, by the sensitivity of the photocathode within the streak camera. The transfer function of the optical path was determined by measuring the transmissive characteristics of each element using a Perkin-Elmer Lambda 9 Spectrophotometer [2]. The resulting function is multiplied by the efficiency of the photocathode [1] to determine the response illustrated in Fig. 2. Both spectrally integrated (brightness) and two-color measurements have been made over a portion of the field of view by employing a color-glass filter with a threshold at 590 nm. The filter isolates the contributions of the two distinct regions of sensitivity illustrated in Fig. 2 without requiring separate detectors.

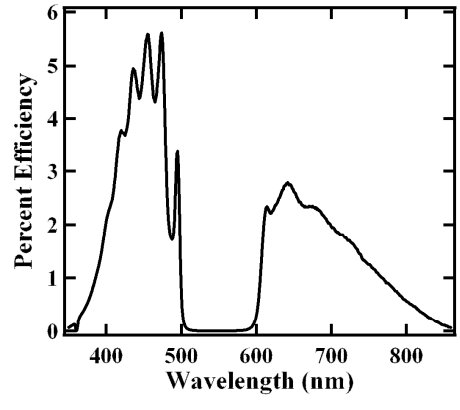

FIGURE 2. Total calculated spectral response of the pyrometer, S(λ), after losses through the optical path and photocathode of the streak camera, expressed as a percentage of emitted light from the sample. The gap between 500 and 600 nm is caused by the dichroic beamsplitter that separates the VISAR signal at 532 nm.

Current experiments are underway to perform spectrally-resolved pyrometry interchangeably with the spatially-resolved configuration described here.

Calibration Technique

Calibration is similar to that described by Miller et al. [3]. Absolute temperatures are extracted from the streak records assuming grey-body behavior through comparison with a NIST traceable standard of known spectral radiance (Optronics Laboratories, OL550 tungsten ribbon filament, [4]). Temperature is related to spectral radiance via Planck's law

$$L(\lambda,T) = \varepsilon \frac{2hc^2}{\lambda^5} \frac{1}{e^{hc/\lambda kT} - 1} \qquad (1)$$

where h, c and k are Planck's constant, the speed of light and Boltzmann's constant, respectively, λ is the wavelength and T is the temperature of the body. The emissivity, ε, is given by Kirchoff's law as $(1\text{-}R(t))$, where $R(t)$ is the reflectivity of the sample at time t , and is measured separately.

The number of recorded counts, $I(T)$, on the detector is proportional to $L(\lambda, T)$, with the proportionality determined by the system response illustrated in Fig. 2, and a number of adjustable parameters. These include the voltage across the camera's micro-channel plate (gain), the detector's opening aperture, CCD exposure time and streak length. The influence of each of these parameters on the number of observed counts is calibrated individually, using the same tungsten ribbon filament. A set of scaling terms, denoted C in Equation 2, is thus determined for a given experimental configuration such that

$$I(T) \equiv C \int S(\lambda) L(\lambda,T) d\lambda \qquad (2).$$

The pyrometer is capable of observing temperatures below 4000K, more sensitive than the best available pyrometer currently used on laser-driven compression experiments [3]. This increased sensitivity is ideal for observation of high-pressure melt transitions in condensed matter.

Uncertainties in temperature are dominated by our inability to determine ε and the absorptive behavior of the sample over the spectral response of the pyrometer. Temporally evolving, wavelength-dependent changes in the optical properties of the sample may effectively alter the measurement of the thermal emission and lead to erroneous temperature values. This has motivated the development of a broadband reflectivity diagnostic to improve our understanding of the optical properties of compressed materials.

Broadband Reflectivity

Reflectivity measurements provide a means of probing the electronic structure of condensed matter. We have successfully demonstrated a temporally-resolved broadband reflectivity diagnostic using high-intensity, non-linear pumping of a standard optical fiber (Fig. 3). This diagnostic responds to the need for a sufficiently bright white-light source for high energy-density measurements on nanosecond time scales.

In these experiments, a ~10 ns FWHM pulse from a 532 nm, Q-switched Nd:YAG laser is injected into a 23 meter, 50 μm diameter silica-core multimode fiber. Non-linear optical effects, including stimulated Raman scattering, four-wave mixing and self-phase modulation, lead to spectral broadening of the injected pulse [5, 6, 7] and thus to an emission of light spanning a wavelength range of about 350 nm (Fig. 4).

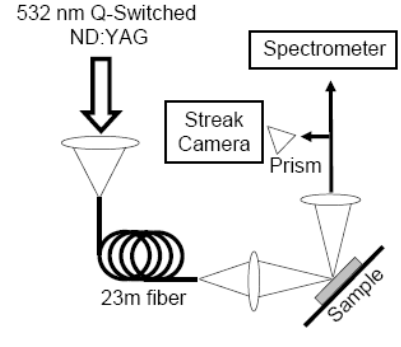

FIGURE 3. Supercontinuum generation by nonlinear effects in the optical fiber results in broadband output that is used to make temporally-resolved reflectivity measurements of the sample.

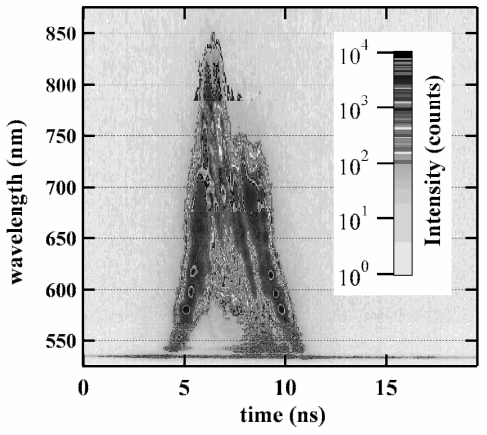

FIGURE 4. Example of the spectrum generated with the system described above, reflected from a target at ambient pressure. Spectral broadening begins from the pump wavelength (532 nm), and extends to an upper limit determined by the sensitivity of the streak camera photocathode near 850-875nm. Efforts are underway to mitigate the observed time-dependence of the spectrum, which results from the same non-linear processes responsible for the supercontinuum.

This white-light (supercontinuum) pulse is reflected off the sample at 27 degree incidence during dynamic loading. The reflected light is collected and spectrally dispersed by a prism, before being directed onto a streak camera. Changes in reflectivity can thus be observed simultaneously with VISAR, permitting direct correlation between the two data sets. An additional spectrometer (Acton SpectraPro 2300i) yields a time integrated spectrum for comparison with the streaked spectrum and to aid with calibration. In initial tests, a 150 μJ injected pulse was sufficient to recover ~27 μJ at the detector, for an efficiency of approximately 18% which is more than adequate to study material properties over the nanosecond timescales characteristic of laser-driven compression experiments.

This new diagnostic greatly expands upon previous single-wavelength measurements using the VISAR probe beam and can serve to constrain wavelength-dependent emissivity over the spectral range observed by the pyrometer described above.

CONCLUSIONS

Two new diagnostics have been developed for the Janus laser facility to probe the thermal and optical properties of materials at high temperatures and pressures. Both single- and two-color pyrometry has been successfully demonstrated for ramp compression as well as shock loading. In addition, a nanosecond broadband reflectivity diagnostic now allows characterization of the optical properties of materials over a nearly 350 nm wavelength range with high temporal resolution. Together with existing VISAR capabilities, these tools allow the possibility of robust P-V-T equation of state experiments and material studies at multi-Mbar dynamic pressures.

ACKNOWLEDGEMENTS

Kjell Tengesdal (LLNL) acquired equipment and assisted in setting up the broadband reflectivity diagnostic. Dylan Spaulding works under the support of a Krell Institute DOE/NNSA Stockpile Stewardship Graduate Fellowship. This work was performed under the auspices of the U.S. DOE by LLNL under Contract No. W-7405-ENG-48.

REFERENCES

1. High Dynamic Range Streak Camera C7700 Instruction Manual and Test Report, Ver.1.3, 2006.7, 6660-401-02, Hamamatsu Photonic Systems, Bridgewater, N.J., 08807-0910.
2. Lambda 9 Specification Manual, Perkin Elmer Corp., Norwalk, CT, 06859-0010.
3. Miller, J.E. et al., Review of Scientific Instruments **78**, 034903 (2007)
4. OL Series 550 Standards of Spectral Radiance with Sapphire Windows, Specification Manual, Optronic Laboratories, Inc., Orlando, FL 32811.
5. Dudley, J.M., Genty, G., Coen, S., Supercontinuum Generation in Photonic Crystal Fiber, Rev. of Modern Physics, Volume **78**, Oct-Dec 2006.
6. Gordon, J.P, Theory of the Soliton Self-Frequency Shift, Optics Letters, Vol. **11**, No. 10, 662-664 (1986)
7. Mitschke, F.M., Mollenauer, L.F., Discovery of the Soliton Self-Frequency Shift, Optics Letters, Vol. **11**, No. 10, 659-661 (1986)